

## Investigation of the Capacity of Braced Slender Reinforced Concrete Columns

Ramez Raafat Sadek<sup>1</sup>, Ayman Abo El Fotouh Embaby<sup>2</sup>, Ayman Hussein Khalil<sup>3</sup>

<sup>1</sup>(B.Sc., Structural Engineering Department, Ain Shams University, Cairo, Egypt)

<sup>2</sup>(Professor of Concrete Structures, Structural Engineering Department, Ain Shams University, Cairo, Egypt)

<sup>3</sup>(Professor of Concrete Structures, Structural Engineering Department, Ain Shams University, Cairo, Egypt)

**Abstract:** The use of slender concrete columns has been of a significant rise lately, with the affordability & availability of high-strength concrete, and the advancement of design methods. Despite this trend, the design provisions for the slender columns haven't been changed significantly since its inception. Better understanding, as well as improved design provisions, for the slender concrete columns can allow for extended use whereas maintaining safety. The objective of this research is an improved understanding of the slender concrete column's behavior and limits, and to develop an improved procedure, in order to be incorporated into building codes. In this paper, a parametric study of 2520 specimens using analytical software shall be presented to exhibit behavior of braced slender concrete columns. Also, several portions of the slender column provisions in the Eurocode are of interest for advancement. A new method will be offered aiming to correct the Eurocode's nominal curvature method which underestimates the columns curvatures under the balance loads. Also, various code provisions and methods that predict the behavior of the slender concrete columns, will be put to comparison. The studies shall include isolated and braced slender concrete columns.

**Key Words:** Braced slender concrete columns, Isolated slender concrete columns, P-delta effect, Curvature, Finite Element Model, Frame Element, Layered Shell Element

Date of Submission: 21-03-2020

Date of Acceptance: 07-04-2020

### I. Introduction

This report addresses the P-delta effect of the slender braced concrete columns. Slender columns are subjected to additional moments due to their lateral deflections. These moments cause a reduction in the axial-load capacity of the column. In first-order analysis, the effect of the deformations on the internal forces in the members is neglected. In second-order analysis, the structure's deformed shape is considered in the equilibrium equations. Most of the computer programs and engineering calculations are based on first-order analyses, results of first-order analysis were modified by several methods to account for the second-order effects. Many codes use approximate equations to compute additional moment for the slender columns to account for the second order effects. The second order effects can be significant, and designers must account for them when designing compression members. There are two types of second-order effects: global effects ( $P\Delta$ ) and member effects ( $P\delta$ ). Global effects are most associated with sway effects, where the deflection of the end points of members cause increased second order effects. On the other hand, interstorey effects are usually associated with non-sway effects, where deflection between the member endpoints causes increased demands. This aim of this paper is to create a parametric study using analytical modelling, to exhibit the non-linear behavior of the braced slender column when loaded with an eccentric axial load, but first the analytical model needs to be verified. Several experimental works have been chosen, and the analytical model shall be tested against their results. Also, the Eurocode's nominal curvature method is under question in this paper. As shown in Figure 1, under the balance load, the curvature relation is assumed as a vertical straight line which is not correct, when compared to the exact curvature calculated for the column. The exact curvature can reach up to several times higher than that of the Eurocode. This may result to failure in slender columns through the design process. The equations which account for the additional moments in different codes, as well as their basics and assumptions shall be discussed. This paper shall offer a brief description of several code provisions including (ECP 08, ACI 318, Eurocode 02, and BS8110) and the literature shall discuss the works investigated by various researchers.

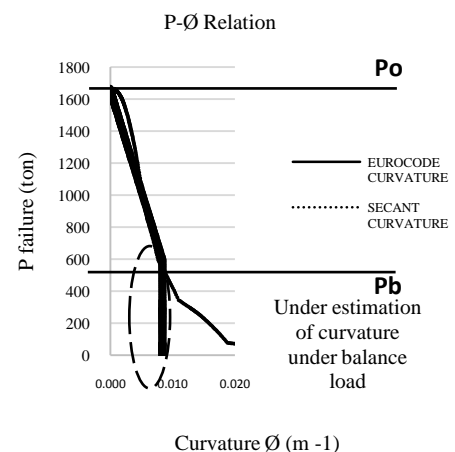


Figure 1 - P-Ø Relation

(Paul Frost) studied the methodologies of Nominal Stiffness and Nominal curvature found in Eurocode-2 for the second order effects in columns. Creep ( $\phi_{ef}$ ) and slenderness ( $\lambda$ ) effect on the second order moments have been studied. For the Nominal Stiffness method, creep has an ascending influence as the slenderness ratio increases. For the Nominal Curvature method, it has been determined that creep has an influence under a certain threshold value of  $\lambda$ . It can also be concluded that in general both simplified methods give similar results for second order moments, but when including creep in the calculations the Nominal Stiffness method gives slightly higher  $M_2$  values for columns with higher slenderness value than the permissible limit. In very slender columns adding reinforcement doesn't allow to neglect second order effects, but for columns just over the slenderness limit it could be a valid option. Increasing the cross-section size reduces second order effects substantially. A spreadsheet was created to ease the Simplified Methods calculation. To assess the behavior of the  $M_2$  vs  $\lambda$  curves obtained through the simplified methods, multiple columns with ranging lengths have been modeled and analyzed through the FEM program (Diana). The results show that the simplified methods give slightly higher second order moments than in the finite element simulations, which indicates that the simplified methods of Eurocode-2 tend to give more safe and conservative values for the second order effects.

In a study by (Timo K. Tikka & S. Ali Mirza), 2,960 simple braced frames were investigated, different methods of calculating the effective length K factor were used while computing their strength. A comparison between the theoretical computed column strengths and the ACI moment magnifier method was held, using different combinations of equations for K and EI. In order to obtain the dimensionless strength ratios, the theoretical computed column strengths were divided by the strength's obtained from the ACI moment magnifier method using different combinations of K and EI equations. A nonlinear EI equation was proposed by Tikka and Mirza, to replace the ACI (EI) equation which was proven to improve the computational accuracy of the moment magnifier method.

(M. A. Farouk) Investigated second- order analysis in braced slender columns, two main points were considered. Firstly, is computing the additional moments in slender columns according to equations accredited in different codes as well as their basics. Secondly, to compute the additional moments in slender columns, an approximate equation was suggested. For elastic analysis, this equation was proved and for single curvature cases as well. the column supported on two pin supports with rotational springs at its ends. The induced additional moments in the slender column were considered, not only in the column's mid span, but also the connected beam's rigidity and the additional moments induced between them and the column. The purpose of the rotational spring is to consider the connectivity of the beams with the column. Upon comparing the results between, the suggested equation and the finite element results, they both gave matching values.

An axial load-curvature relationship was proposed by (A. Embaby) for axially loaded element to rationalize the determination of columns mid-height deflection, assuming a sinusoidal deflected shape along with satisfying both compatibility and equilibrium conditions:

$$\phi = \frac{P_0 - P}{P_0 - P_b} \phi_b \text{ where } P_b \leq P \leq P_0 \qquad \phi = \alpha P + \beta P^2 + \gamma \text{ where } P \leq P_b$$

The first part of the equation is the same as the Eurocode, but the second part is a second-degree equation to represent the correct behavior of columns under the balanced loads

The correct curvature can be seen in **Figure 3**, in which the euro code has a straight-line relationship, while the curvature value is much higher, also in **Figure 2**, the Eurocode overestimates the failure loads due to the underestimated curvature values

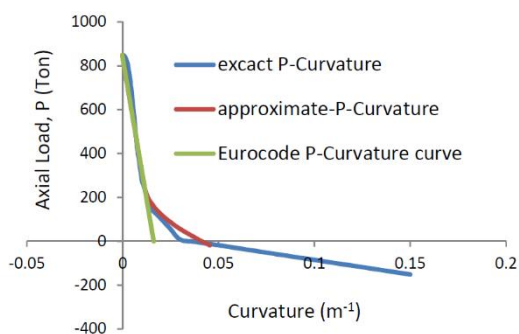


**Figure 3 - Axial Load – Curvature Relationship**

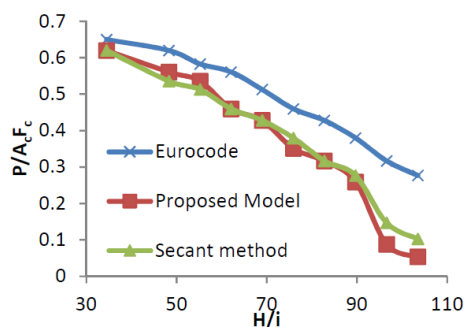


**Figure 2 - Normalized Failure Loads Against Slenderness Ratio**

## II. Numerical Modeling for Isolated Columns

The following section describes the proposed finite element modeling using the SAP 2000 software. The necessary steps needed to create the models which will investigate the slender column behavior will be discussed. The objective of the forthcoming section is to create a comparison between the numerical results from SAP 2000 using two methods, The Frame element and The Layered shell element. These two methods will be compared with the experimental results of the concrete rectangular specimens, collected from experimental works (Tim Gudmand-Høyer & Lars Zenke Hansen). The aim is to find the best modeling technique for the numerical model, results will be plotted against each other to see which method has a better representation of the experimental results. The Nonlinearity of structural system is due to material nonlinearity as well as geometric non-linearity. Material strengths and moduli of elasticity of the concrete and rebar were defined into the software. A single load pattern was defined for each specimen, self-weight of the specimen was ignored.

**The Frame Element:** The column is modeled as shown in Figure 4. A single frame element with five predefined locations of plastic hinges has been used. The calculated reinforcement was defined to match the experimental data. The boundary conditions were selected to model a 2D braced columns, through appropriate restricted degrees of freedom. The vertical load is applied to the column's top joint, moments are applied to both top and bottom joints. The moment's directions applied aims to create a single curvature bending moment with eccentricity equivalent to that of the experimental works.

**The Layered Shell element:** As an another modeling alternative, the column was modeled using the layered shell element in which the shell thickness was divided into multiple layers, 4 for concrete, and 2 layers for reinforcement, the column width was divided to 2 shell element. The boundary conditions are kept the same as the frame element. The material nonlinearity was considered for both materials, also the geometric nonlinearity was also considered by activating large displacement - large rotation analysis option in SAP 2000. The applied load is shown in Figure 5. single curvature moment was applied to the column.

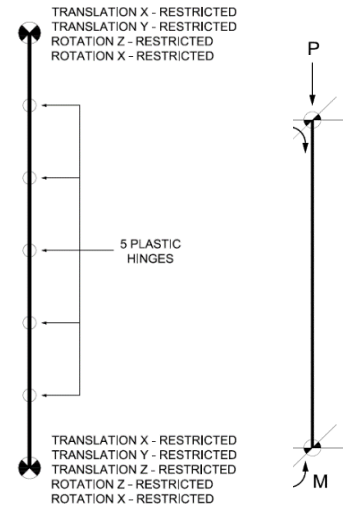


Figure 4 – Frame Element

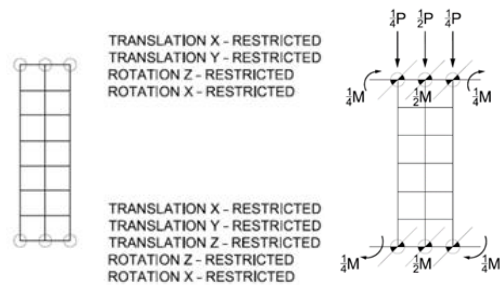
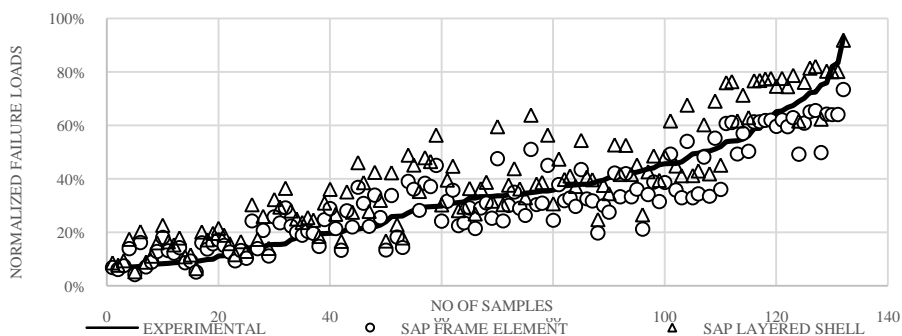


Figure 5 - Layered Shell Element

The experimental works contained 132 test results works. All the specimens are rectangular columns. Sizes of the specimens ranged from 10 cm up to 25 cm. Slenderness ratios of the specimens ranged from 10 up to 140. Concrete strength ranged from 16 Mpa up to 90 Mpa. Reinforcement yield strength ranged from 270 Mpa up to 680 Mpa. Reinforcement ratio ranged from 0.6 % up to 4 % .  $e/t$  ratio ranged from 0.1 up to 1.8. All the tests were treated as isolated hinged-hinged fixations (no moments induced at column ends). The normalized failure load is the division of a given method's failure load by the pure axial failure load of the column (considering zero moment and eccentricity).

The following plot shows the normalized failure loads in comparison to each other, between the experimental works and the numerical model results. The numerical model adequately represents the experimental works. It should be noted that the frame element was relatively close results to the experimental results than the layered shell element.



### III. Parametric Study for Braced Slender Concrete Columns

This section discusses the behavior of braced slender concrete columns subjected to eccentric axial loads. In order to represent a generalized slender braced concrete column, the following frame shape has been assumed, see Figure 6, an intermediate story column, in the middle of a building, in which the degrees of freedom permitted are as follows: Joint A is restricted by an in plane rotational spring. Joint B is restricted by spring for in plane rotation along with hinge restricting vertical translation. All out of plane degrees of freedom, and torsional movements were restricted. Various controlling parameters have been chosen throughout this study. A square cross-section column with a 60 x 60 cm size was chosen.

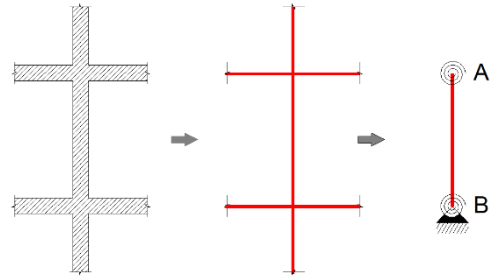


Figure 6 -Frame Representation in Analytical Model

**Testing Matrix:** The chosen parameters are as follows:

1.  $\Psi$  is a factor representing the rigidity (stiffness) of the beams connected to the column, as per the Jackson Moreland logarithmic alignment chart in Figure 7. Values are chosen as follows 0, 0.2, 0.5, 1, 5, 50 and  $\infty$ , ranging from a fixed end to a hinged end. Fixed end meaning that the bracing elements (beams) are very stiff in comparison to the column and vice versa. The chosen values aim to capture all cases of fixity a column may be subjected to.  $\Psi$  is calculated at each column end using this equation  $\Psi = \sum \frac{EI}{L_c} / \sum \frac{EI}{L_b}$ , so that the effective length can be calculated.
2.  $\lambda$  is a factor representing the slenderness ratio for columns, or in other words the column's length, supposing a constant cross-section. Values are chosen as 40, 60, 80, 100, 120 and 140.  $\lambda = L/r$ , in which L is the column's length, and r is the radius of gyration.
3.  $\rho$  is a factor representing the column's reinforcement ratio, ratios are equal to 1%, 2%, 3% and 4%, reinforcement value  $A_s = A_c * \rho$
4.  $\beta$  is a factor representing the applied load which is the e/t ratio, this describes how far is the load applied from the column's centroid, see Figure 9, as e/t ratio increases, the induced moment on the cross-section increases. Ratios are equal to 0.1, 0.2, 0.3, 0.4 and 0.5.
5.  $C_m$  is a factor representing the variation of the moment through the column's height, in which  $C_m = M_1/M_2$ , see Figure 8.  
 $C_m = (-1 / 0 / 1)$  in which:  
 (-1) → Double Curvature  
 (0) → Triangular Single Curvature  
 (1) → Constant single curvature

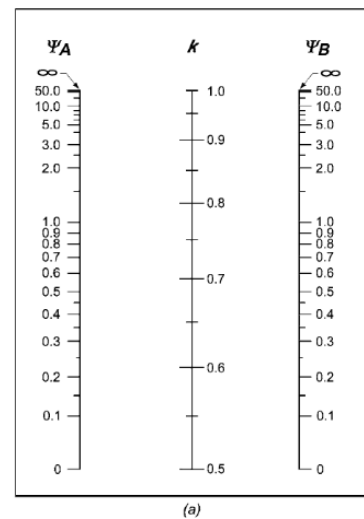


Figure 7 - Jackson Moreland Alignment Chart for Braced Columns

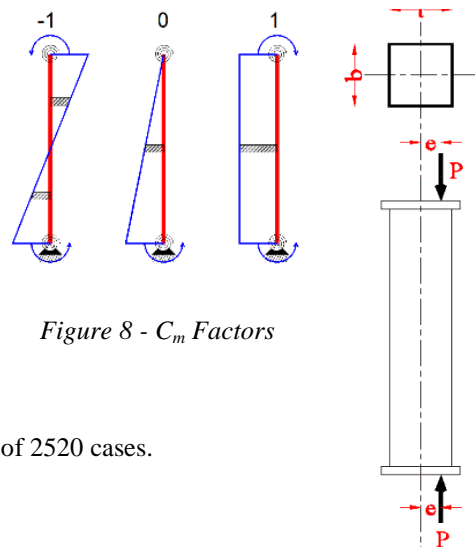
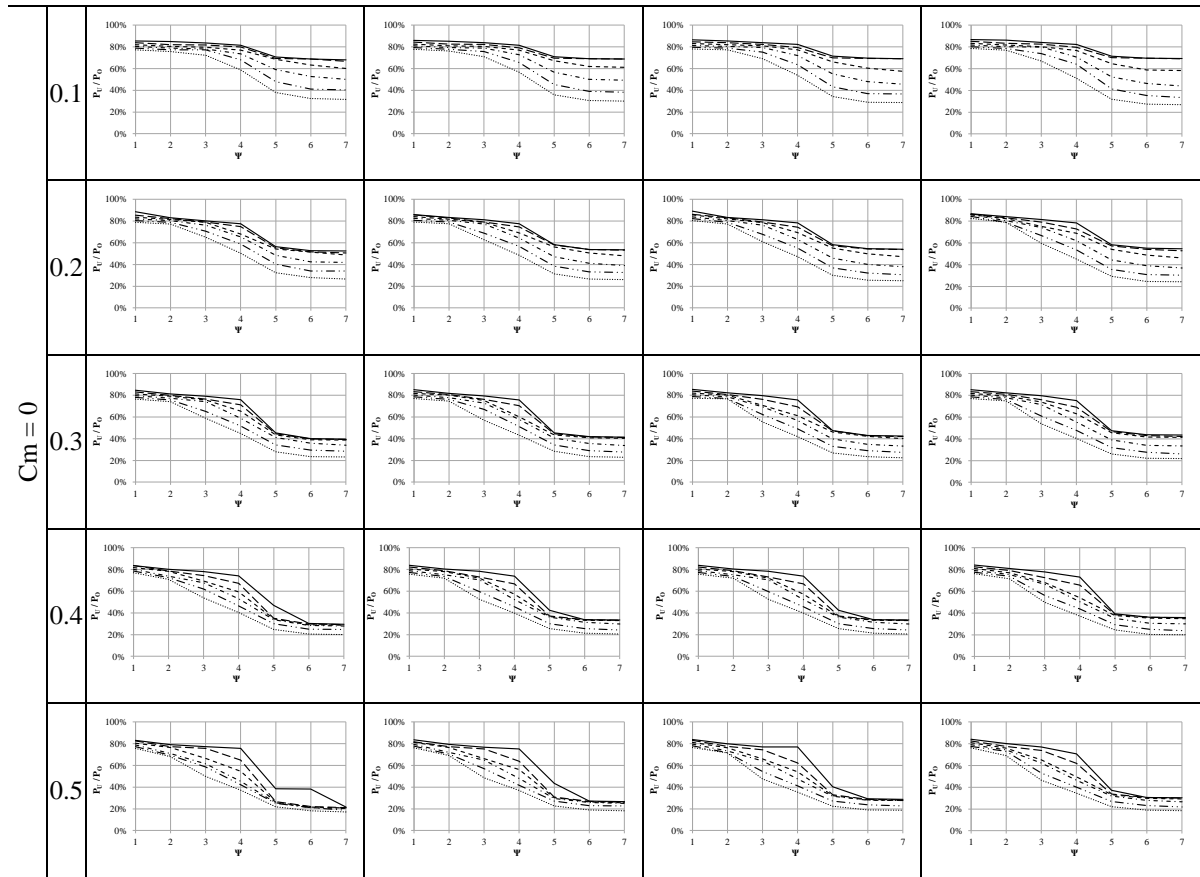
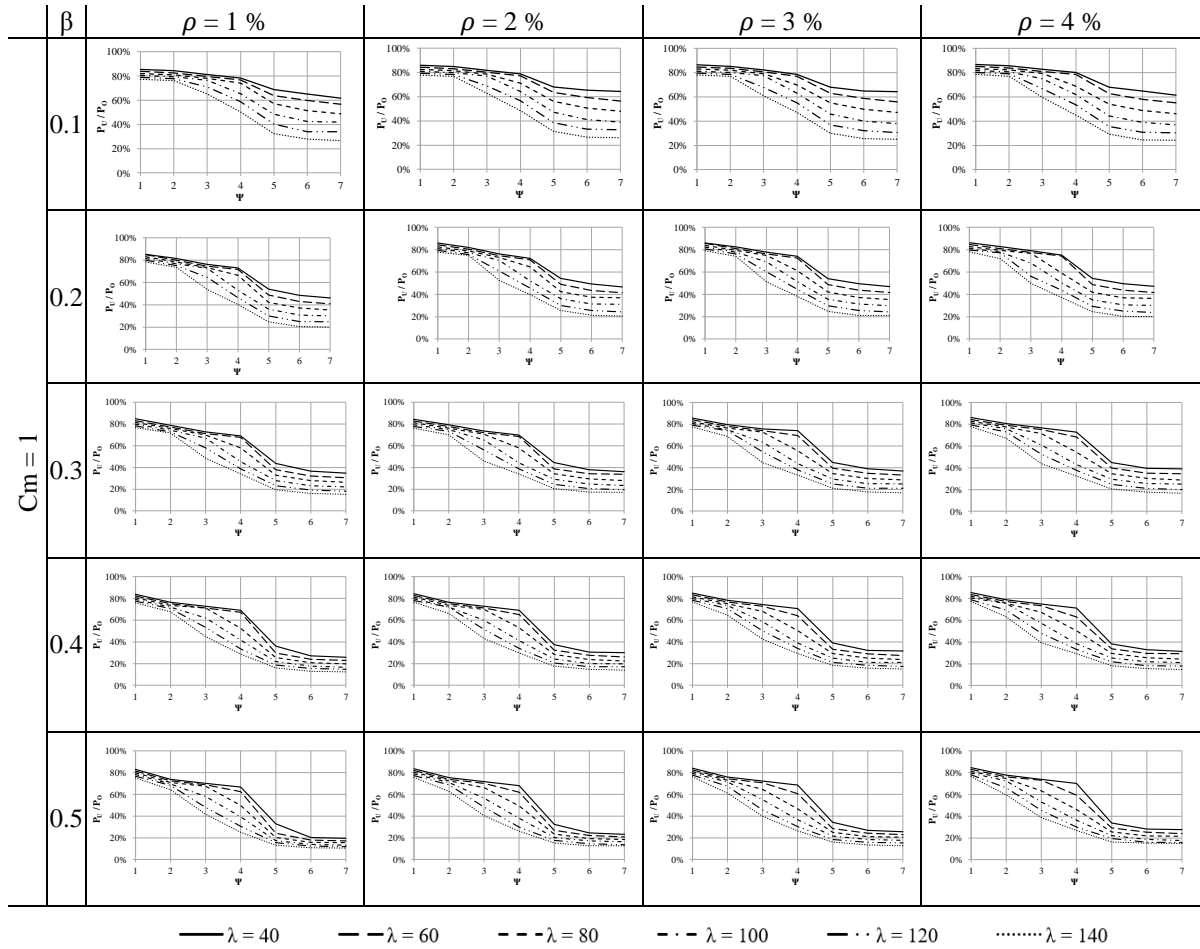


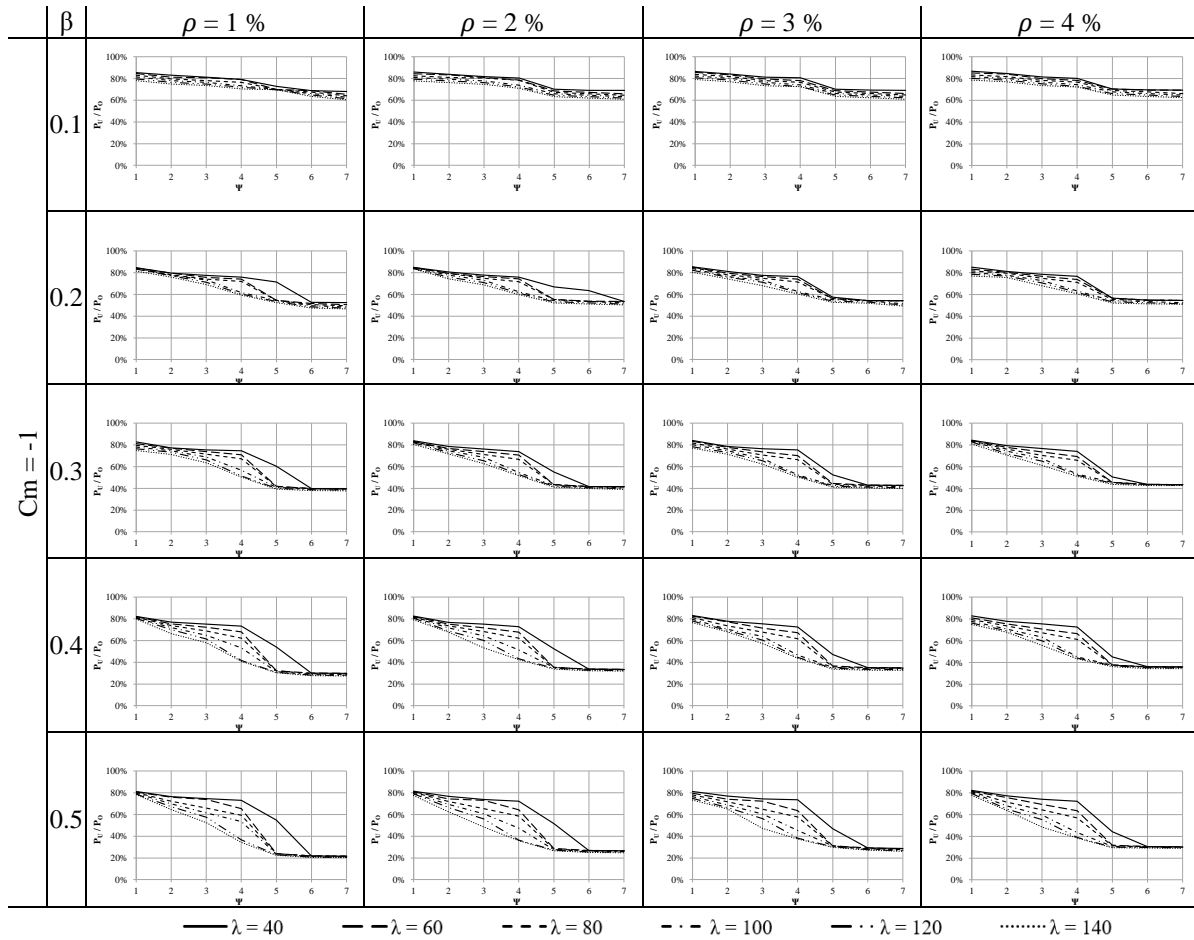
Figure 8 -  $C_m$  Factors

From the above varying parameters, this testing matrix shall consist of 2520 cases. Concrete strength ( $F'_c$ ) values were set to a constant 40 Mpa. Rebar strength ( $F_y$ ) values were set to constant 400 Mpa. A 60 x 60 cm. column was used throughout the study.

Figure 9 e/t ratio

*Investigation of the Capacity of Braced Slender Reinforced Concrete Columns*





**Discussion & Commentary:** The previous plotted graphs are a result of 2520 specimens, tested analytically using SAP 2000. The plotted graphs were categorized into three main groups, which are the three loading patterns ( $C_m$ ) (Constant single curvature - Triangular single curvature - Double curvature).

On each graph, the X – axis contains the  $\Psi$  values, with numbers ranging from 1 to 7, the 1, being a fully fixed end, to 7, a pure hinged end, while the Y – axis contains the normalized failure loads, which is the failure load of the column obtained from the analytical model divided by the pure axial capacity of the cross-section  $P_o$ .

$$[P_o = A_c * F'_c + A_s * F_y]$$

All of the parameters included in this study affect the SAP failure load results, except for the reinforcement ratio  $\rho$ , which affects both values of SAP and the  $P_o$ , therefore the results will be more challenging when trying to interpret and conclude the column's behavior.

**Effect of moment application direction ( $C_m$ ):**

$\Psi$	1			7		
$C_m$	1	0	-1	1	0	-1
Normalized Failure Load	85%	85%	85%	29%	36%	45%

When observing the  $C_m$  variation, it can be seen that at the fixed state, the moment directions aren't of significance on the failure loads, but when the case is hinged, the case is entirely different, the constant single curvature resulted at the most extreme loading, thus the lowest failure load, followed by the triangular curvature, and lastly the double curvature loading pattern.

$\Psi$	6																							
$\rho$	1%						4%																	
$\beta$	0.1			0.5			0.1			0.5														
$\lambda$	60		120	60		120	60		120	60		120												
$C_m$	1	0	-1	1	0	-1	1	0	-1	1	0	-1	1	0	-1	1	0	-1						
Norm. Failure Load	0.60	0.69	0.69	0.34	0.41	0.69	0.18	0.22	0.22	0.12	0.21	0.22	0.58	0.70	0.69	0.31	0.35	0.69	0.25	0.31	0.31	0.16	0.23	0.31
Ratio	0.87	1.00	1.00	0.50	0.60	1.00	0.82	1.00	1.00	0.57	0.96	1.00	0.83	1.00	1.00	0.45	0.51	1.00	0.83	1.00	1.00	0.52	0.76	1.00

When focusing on the hinged state columns (6), where the moment application direction showed a significant variation, it can be seen that:

The shorter columns group have the same results for the triangular and double curvature cases, but for the longer columns, the moment directions had a significant effect.

The difference in eccentric loading didn't have much of a difference in results except for the longer columns.

The difference in reinforcement ratio didn't have much of a difference in the results.

**Effect of Loading Factor ( $\beta$ ):**

It can be noticed that as the eccentric load increases, there is a general decrease in the failure load of all specimens, which is expected, because as the eccentricity increases, moments increase, therefore a lower failure load.

Upon taking a closer look to the results, especially upper and lower bounds of the results.

Cm	1.00							
$\rho$	1.00%							
$\lambda$	40				120			
$\psi$	1		7		1		7	
Specimen No	0.1	0.5	0.1	0.5	0.1	0.5	0.1	0.5
Normalized Failure Load	86%	83%	62%	19%	85%	84%	34%	12%
% of Variation	3.4%		69.3%		1.1%		64%	

C<sub>m</sub> was chosen as the constant single curvature and the reinforcement ratio as 1%, as these are the most extreme cases, two slenderness values have been selected 40 & 120, also two fixity values of 1 & 7.

As the  $\beta$  value increases, the amount of the normalized failure load decrease is very dependent on the fixation mode:

For  $\lambda = 40$ , the fixed state shows a 3.4% difference in load values, while in the hinged state, there is a difference of 69.3%.

For  $\lambda = 120$ , the fixed state shows a 1.1% difference in load values, while in the hinged state, there is a difference of 64%.

It can be concluded that as the stiffness of the beams connected to the column increases, the difference percentage between the normalized failure load decreases.

**Effect of Slenderness Ratio ( $\lambda$ ):**

Cm	1											
$\rho$	2%											
$\beta$	0.3											
$\psi$	1						7					
$\lambda$	40	60	80	100	120	140	40	60	80	100	120	140
Normalized Failure Load	86%	86%	86%	86%	85%	83%	36%	34%	28%	23%	20%	17%

It is expected, that increasing the column's length decreases column's strength, however this decrease was pretty significant at the hinged end columns, and not so much at the fixed columns.

As it can be seen in the table above the decrease in strength in the fixed end columns, is very small, and in the small slenderness ratio, the column's achieved the same failure load, which can be attributed to the fact that, that column is not slender enough to exhibit the non-linear behavior.

As for the hinged end columns, the decrease of the strength is significant.

**Effect of Reinforcement ( $\rho$ ):**

Cm	1							
$\beta$	0.5							
$\lambda$	60				120			
$\psi$	1		7		1		7	
$\rho$	1%	4%	1%	4%	1%	4%	1%	4%
Normalized Failure Load	84%	86%	17%	24%	84%	84%	12%	16%

It is expected that increasing the reinforcement ratio, increases the failure load of the column, so partially the normalized failure loads, should be close to each other as the P<sub>o</sub> -as mentioned earlier- contains the reinforcement percentage as a factor. It can be noticed that the normalized failure load increased slightly with the increase of the reinforcement. At the fixed state columns, the increase was slight, around 2%, but for the hinged state, the increase was higher, around 41%. For the shorter column, the increase was around 41%, but for the longer columns, the increase was less, around 33%

**Effect of Fixation Strength ( $\Psi$ ):**

Cm	1													
$\rho$	2%													
$\beta$	0.3													
$\lambda$	60							120						
$\psi$	1	2	3	4	5	6	7	1	2	3	4	5	6	7
Normalized Failure Load	86%	84%	82%	71%	39%	34%	34%	85%	75%	56%	39%	25%	21%	20%
Ratio	1	0.98	0.96	0.82	0.45	0.40	0.39	1	0.89	0.66	0.46	0.29	0.24	0.23

As expected, as the effect of fixation increases, the failure load increases.

For longer columns, the decrease of the failure load is much larger than that of the shorter ones.

#### IV. Simplified Model

A simplified mechanistic model had been developed using Excel, this model calculates the failure load of any eccentric loaded column in which several inputs are defined in the model such as:

1. Dimensions (Breadth – Depth - Height)
2. Material strengths ( $F'_c - F_y$ )
3. Applied  $e/t$  ratio
4. Exact reinforcement and distribution
5. Boundary conditions (Hinged or Fixed, attachment to beams)

The model accounts for the geometric non-linearity and gives the failure load of the column at the specified eccentric ratio, the model was originally created by A.E., and later modified and updated by the Author.

The objective of this section is to create a comparison through graph plots, which will compare several code propositions against other methods proposed by the author through the model, the graph plots shall include, the normalized failure loads of the braced concrete columns, through varying parameters, the three codes that are going to be utilized in the calculations are the (Eurocode – ACI – ECP), these code equations are inserted into the mechanistic model calculations, the model also adopts the equations of three design methods which estimate the column's curvature and their failure loads, which are:

1. Secant Method
2. Approximate Method (A.E.)
3. Proposed Method (Author)

The comparison aims to exhibit the behavior of slender braced concrete column under the varying parameters, which were discussed in the previous section, and also through the above-mentioned different methods and codes.

**Model Operation:** firstly, the previously mentioned factors must be inputted into the model, then the model calculates the exact interaction diagram for the column using the strip method.

**The Strip Method:** the strip method is a method in which the column is divided into several strips, in our model six strips, typically the top and the end strips will have heavy reinforcement compared to the middle, see Figure 10.

**Plotting the Interaction Diagram:** Now that a generic interaction diagram has been comprised for any concrete specimen. This tool can calculate the interaction diagram to any generic shape, square, circle, rectangle, polygon, but of course if the shape is too complex, we may have to increase the no of strips to more than six to handle the changing shape of the specimen. It should be noted that this tool, only creates a single planar (2D) interaction diagram, see Figure 11.

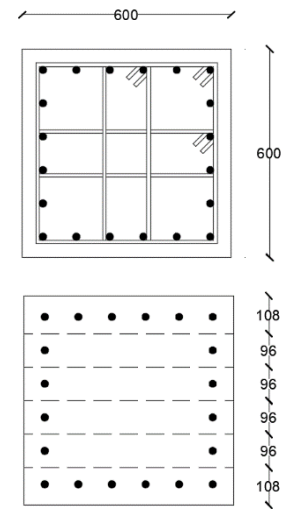


Figure 10 - Concrete Section Strips

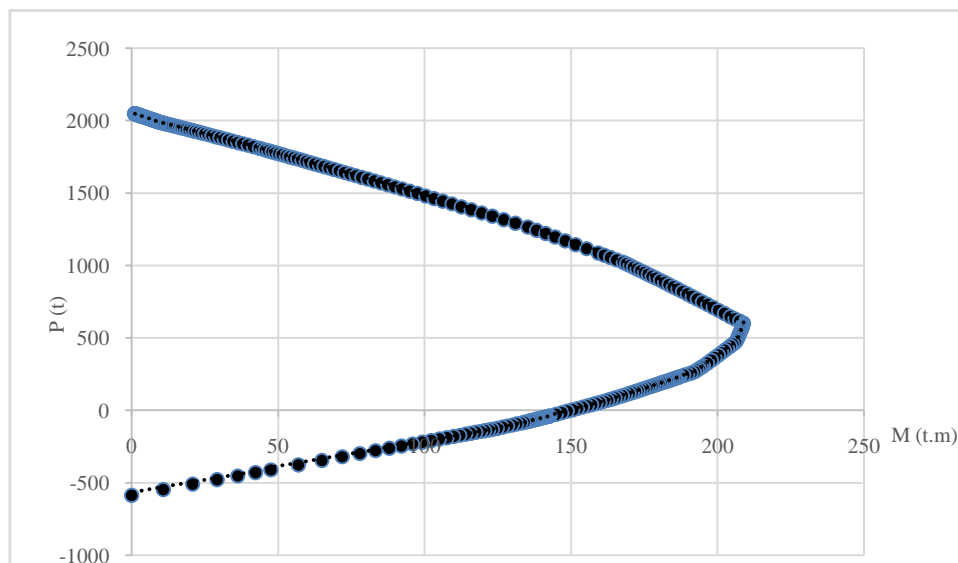


Figure 11 - Typical Interaction Diagram for a RC cross-section.



**Accounting for Geometric Non-Linearity:** Loads acting on the column cross-section are assumed as single bending. Moment bends the column in a single curvature manner. Moment applied on columns consists of two main parts: Moment due to loads and moments due to geometric deformations (geometric nonlinearity)

$$M_{tot} = M_1 + M_{add}$$

$$M_1 = P * \frac{e}{t} * t \text{----- (1)}$$

A sinusoidal deformation of the columns is assumed under the axial's load application see Figure 12.

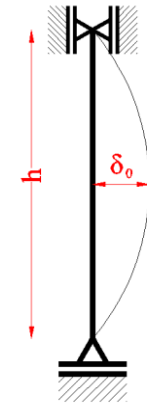
$$y = \delta_0 \text{ SIN} \left( \frac{\pi x}{h} \right)$$

$$y'' = \left( \frac{\pi}{h} \right)^2 \delta_0 \text{ SIN} \left( \frac{\pi x}{h} \right)$$

$$y''_{max} = \left( \frac{\pi}{h} \right)^2 \delta_0$$

$$\delta_0 = \left( \frac{h}{\pi} \right)^2 y''_{MAX}$$

$$\delta_0 = \left( \frac{h}{\pi} \right)^2 \phi$$



In which  $\delta_0$  is the deflection, and  $\phi$  is the curvature

$$M_{add} = P\delta = \left( \frac{h}{\pi} \right)^2 \phi * P \text{----- (2)}$$

From (1), (2)

$$M_{tot} = P * \frac{e}{t} * t + \left( \frac{h}{\pi} \right)^2 \phi * P$$

**Methods Used for Calculating Failure Loads Adopted by the Simplified Model:**

As mentioned previously several codes and methods are inputted into the model, to calculate the column's curvature and its failure loads.

**Secant Method:** At first the exact curvature (secant curvature) is calculated for each point of the Interaction diagram.

$$\text{Curvature } \phi = \frac{\epsilon}{x}$$

In order to obtain the curvature for each point of the interaction diagram, the strain for each point is divided by its distance from the neutral axis.

In which x is the varying distance of the neutral axis application to the last top fiber of the concrete cross-section, see Figure 13.

Figure 12 - Column Deflection

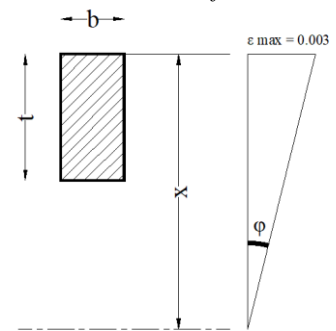


Figure 13 - Secant Curvature Values

**Eurocode (Nominal Curvature Approach):**

This is the curvature calculation inserted into the simplified model.

For  $p < p_{bal}$  the curvature ( $\phi$ ) is constant, as when the  $n > n_{bal}$  the curvature starts to decrease and becomes zero

$p_0$ .

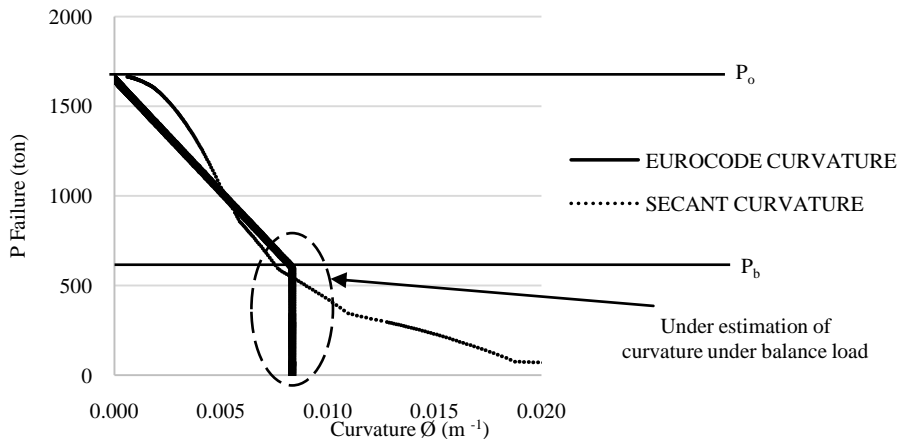


Figure 14 - P-phi Relation for Eurocode

**ECP (BS 8110):**

The ECP code uses a constant curvature value which is independent of the load, see Figure 15.

$$\delta_{\tau} = \lambda^2 * \tau / 2000$$

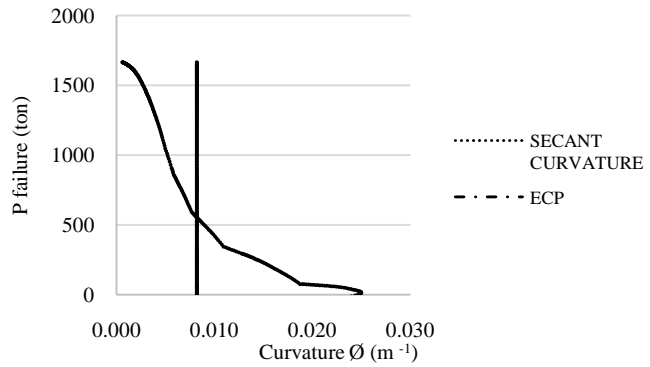


Figure 15 - P-Ø Relation for ECP

**ACI:**

In the American Code, the moment magnifier method is used in the analysis of secondary moments, see Figure 16.

$$C_m = 0.6 + 0.4 \frac{M_1}{M_2}$$

The moment magnifier equation for the cases of no sway is:

$$M_c = \delta_{ns} \cdot M_2$$

The moment  $M_2$  is the greater end moment acting on the column.

$\delta_{ns}$  is taken as follows:

$$\delta_{ns} = \frac{C_m}{1 - \frac{P}{0.75 \cdot P_c}}$$

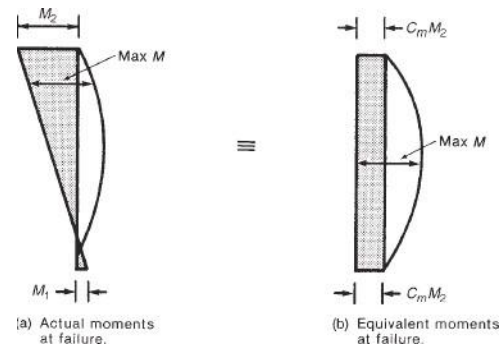


Figure 16 - Moment Redistribution

**The Proposed Method (Author):**

As mentioned previously, a new P- Ø relation was introduced to the model by the author to idealize the nonlinear axial load-curvature. The (P-Ø) curve goes as follows:

$$\delta = \frac{P_0 - P}{P_0 - P_b} \delta_b \text{ in which } P_b \leq P \leq P_0 \quad \text{-----(1) same as Eurocode}$$

$$\delta = \frac{P}{P_b} * (\delta_b - \delta_f) + \delta_f \text{ in which } P \leq P_b \quad \text{-----(2)}$$

The new curvature is a bi-axial relationship, above the balance load, the values are taken as that of the Eurocode's, but under a straight line is connected to the secant curvature value at the pure moment, see Figure 17.

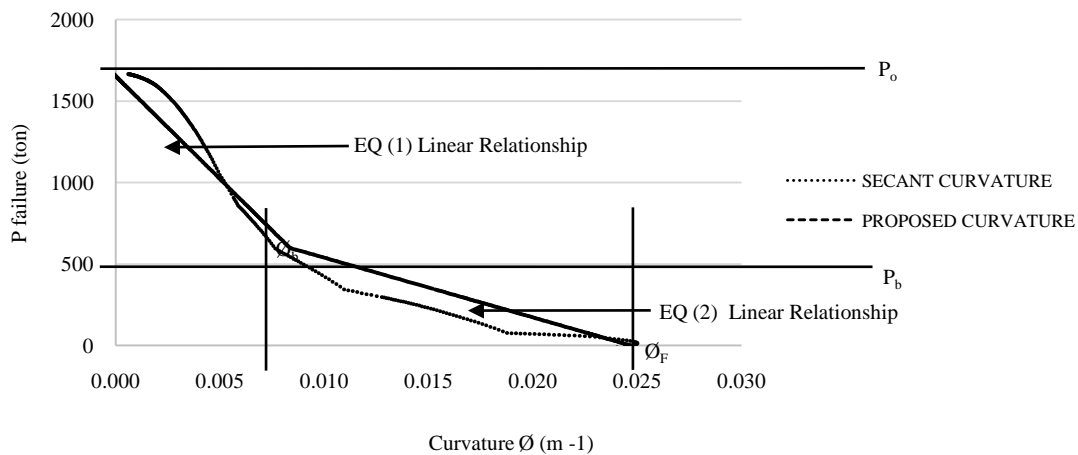


Figure 17 - P-Ø Relation for the Proposed Method

**Consideration of ( $\Psi$ ) in the Simplified Model:**As discussed previously,  $\Psi$  is the factor representing the fixation rigidity for the column, caused by the connecting beams. Connecting the column to beams, can reduce the deflection length of the column, which is called the effective length. In braced members the effective length can range between 0.5 up to 1 of the column's original length, see Figure 18. This depends on the rigidity of the concrete beams bracing the column. The equations used to calculate the effective length is:

$$l_o = 0.5l * \sqrt{\left(1 + \frac{k_1}{0.45 + k_1}\right) * \left(1 + \frac{k_2}{0.45 + k_2}\right)}$$

In the mechanistic model, we swap out the original length of the column, by its effective length or the new reduced length, which will result in a smaller curvature or secondary effect, leading to a higher failure load.

This should represent the effect of the beams bracing the column.

**Testing Matrix:** The same testing matrix used in the parametric

study was utilized. 2520 specimens with varying properties, except this time, failure loads are going to be calculated using the simplified model discussed earlier.

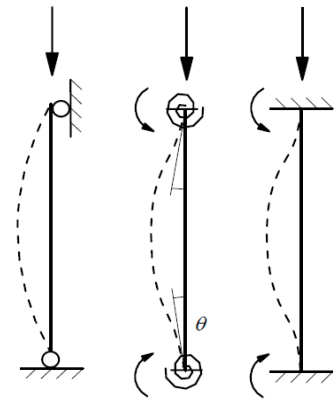
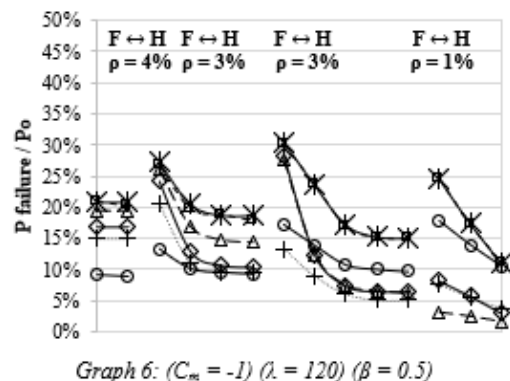
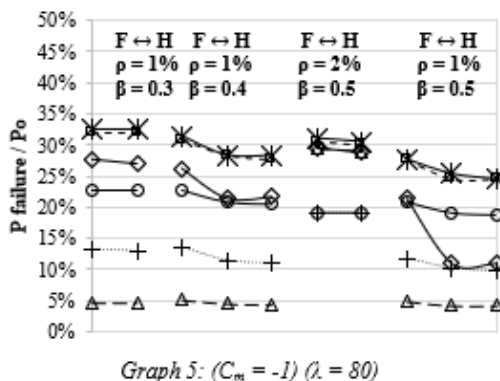
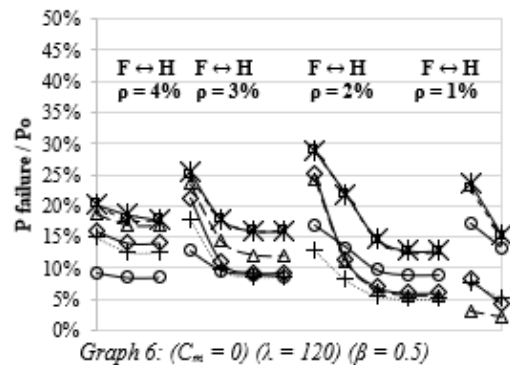
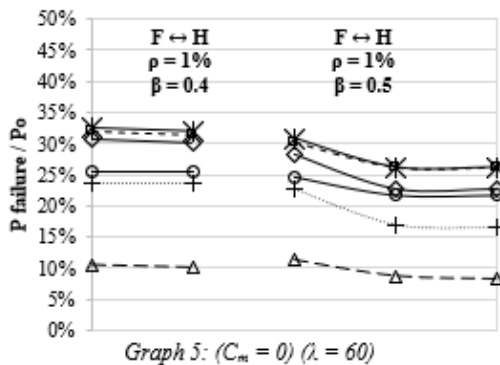
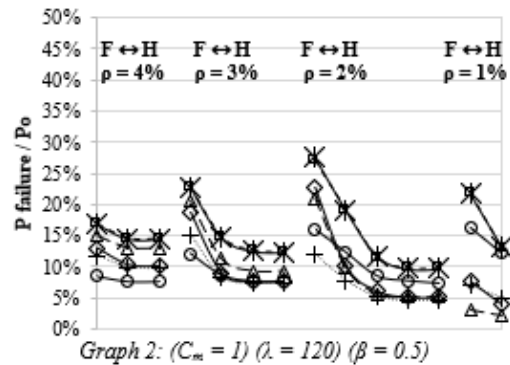
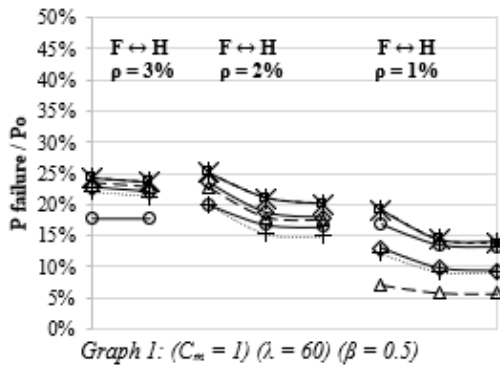


Figure 18: Column Effective Length

**Graphs & Results:**



**Discussion & Commentary:**

The plotted graphs are a sample of the results of 2520 specimens tested by the previously mentioned methods and codes. The plotted graphs were categorized into three main groups, and furtherly more subgroups. The three main groups are the three loading patterns ( $C_m$ ), only slenderness of 60 and 120 were displayed, to exhibit both high and low values of slenderness,  $\beta$  was chosen at the value of 0.5. Inside each graph, each group of lines represent a reinforcement ratio ranging from fixed end specimens to hinged ends.

Methods	Average Normalized Failure Load		
	$C_m = 1$	$C_m = 0$	$C_m = -1$
Secant	13 %	13 %	12 %
Eurocode	<b>20 %</b>	<b>21 %</b>	<b>21 %</b>
Approximate (A.E.)	11 %	11 %	10 %
Proposed (R.R.)	11 %	10 %	9 %
ECP	20 %	21 %	21 %
ACI	13 %	13 %	13 %

In the table above, the shown values are the average normalized failure loads for each ( $C_m$ ). The displayed values show around 30% of the whole testing matrix. Those 30% are the columns highly affected by the second order moments (P-delta). It is noticeable that both the Eurocode and ECP have the highest failure loads of all the methods. It can be seen in the shown P- $\phi$  curve, the Eurocode shows a constant curvature value under the balance load, while the ECP had a constant curvature value generally, which is obsolete. This is why the results showed high failure loads for both the EURO and ECP, the columns second order effects are underestimated, so the failure loads are overestimated. When observing the rest of the methods, all of them resulted in lower failure loads, with behavior close to each other. Each parameter shall be addressed separately.

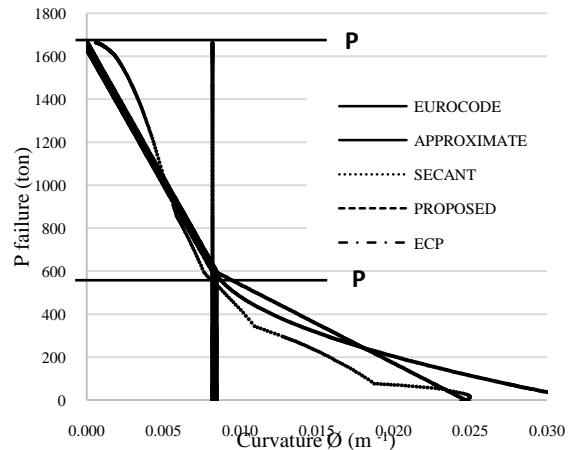


Figure 19 - P- $\phi$  Relation

**Effect of Moment Application Direction ( $C_m$ ):**

$\lambda$	120					
$\beta$	0.3					
$\rho$	2%					
$\psi$	7					
$C_m$	Secant	Euro	Approx.	Prop.	ECP	ACI
1	6.0%	12.5%	5.6%	5.1%	12.8%	8.9%
0	6.9%	15.5%	6.5%	5.6%	15.6%	10.0%
-1	7.3%	17.5%	6.9%	5.6%	17.5%	10.7%
<b>1</b>	<b>1.00</b>	<b>1.00</b>	<b>1.00</b>	<b>1.00</b>	<b>1.00</b>	<b>1.00</b>
<b>0</b>	<b>1.15</b>	<b>1.23</b>	<b>1.17</b>	<b>1.10</b>	<b>1.22</b>	<b>1.13</b>
<b>-1</b>	<b>1.22</b>	<b>1.40</b>	<b>1.25</b>	<b>1.10</b>	<b>1.37</b>	<b>1.21</b>

Values were chosen for the  $\lambda$ ,  $\beta$ ,  $\rho$ ,  $\psi$ , in order to keep track of how the  $C_m$  values affect different methods, in the shaded part of the table, values were divided by each other, to find the percentage of difference between each state. The constant single curvature is shown to be the most severe case of loading, it had the lowest failure loads, followed by the triangular, followed by the double curvature. The Eurocode is the most method affected by the transition of the  $C_m$  from constant single curvature to triangular single curvature with a variation of 23%, while the proposed method showed 10%, as for the transition from the constant single curvature to the double curvature, the value is 40% compared to 10%.

**Effect of Slenderness Ratio ( $\lambda$ ):**

$C_m$	1					
$\beta$	0.3					
$\rho$	2%					
$\psi$	7					
$\lambda$	Secant	Euro	Approx.	Prop.	ECP	ACI
80	20%	24%	19%	13%	24%	16%
100	9%	18%	9%	7%	18%	12%
120	6%	13%	6%	5%	13%	9%
140	4%	9%	4%	3%	9%	7%

As shown in the above table, values were chosen for the  $C_m$ ,  $\beta$ ,  $\rho$ ,  $\psi$ , in order to keep track of how the  $\lambda$  values affect different methods. As the slenderness ratio of the columns increase, the normalized failure load decreases, as  $(P\delta)$  effect appears in longer columns:  $\delta_0 = (h/\pi)^2 \phi$ , both the EURO and the ECP overestimated the failure loads, for all cases of slenderness ratios.

**Effect of Loading Factor ( $\beta$ ):**

$C_m$	1					
$\lambda$	120					
$\rho$	2%					
$\psi$	7					
$\beta$	Secant	Euro	Approx.	Prop.	ECP	ACI
0.1	7.3%	17.9%	6.9%	5.6%	18.3%	10.7%
0.2	6.5%	14.9%	6.0%	5.1%	15.1%	9.6%
0.3	6.0%	12.5%	5.6%	5.1%	12.8%	8.9%
0.4	5.6%	10.7%	5.1%	4.5%	11.0%	8.1%
0.5	5.1%	9.6%	5.1%	4.5%	9.6%	7.3%
<b>0.1</b>	<b>1.45</b>	<b>1.86</b>	<b>1.37</b>	<b>1.23</b>	<b>1.90</b>	<b>1.46</b>
<b>0.2</b>	<b>1.28</b>	<b>1.54</b>	<b>1.19</b>	<b>1.12</b>	<b>1.57</b>	<b>1.31</b>
<b>0.3</b>	<b>1.19</b>	<b>1.30</b>	<b>1.10</b>	<b>1.12</b>	<b>1.33</b>	<b>1.21</b>
<b>0.4</b>	<b>1.10</b>	<b>1.11</b>	<b>1.00</b>	<b>1.00</b>	<b>1.15</b>	<b>1.11</b>
<b>0.5</b>	<b>1.00</b>	<b>1.00</b>	<b>1.00</b>	<b>1.00</b>	<b>1.00</b>	<b>1.00</b>

Values were chosen for the  $C_m$ ,  $\lambda$ ,  $\rho$ ,  $\psi$ , in order to keep track of how the  $\beta$  values affect different, in the shaded part of the table, the values were divided by each other, to find the percentage of difference between each state. Generally, there is a decrease in the failure load as the eccentric load location increases. The Eurocode is highly affected by the transition of the  $\beta$  from (0.5) to (0.1) with a factor of 86%, while the proposed method showed 23%. The ECP was the most affected method with a percentage of 90%.

**Effect of Reinforcement ( $\rho$ ):**

$C_m$	1					
$\lambda$	120					
$\beta$	0.3					
$\psi$	7					
$\rho$	Secant	Euro	Approx.	Prop.	ECP	ACI
2%	6.0%	12.5%	5.6%	5.1%	12.8%	8.9%
3%	9.3%	16.0%	11.9%	8.6%	16.0%	8.6%
4%	14.0%	17.7%	16.8%	12.6%	17.7%	9.0%

Values were chosen for the  $C_m$ ,  $\lambda$ ,  $\beta$ ,  $\psi$ , in order to keep track of how the  $\rho$  values affect different methods. Generally, as the reinforcement ratio increases the normalized failure load increases, values of the Eurocode and the ECP compared to the other methods are higher as the usual case, except for the higher reinforcement specimens, it seems there is a correspondence in the results.

**Effect of Fixation Strength ( $\psi$ ):**

$C_m$	1						
$\lambda$	100						
$\beta$	0.3						
$\rho$	2%						
$\psi$	Secant	Euro	Approx.	Prop.	ECP	ACI	Secant
5	29%	12%	21%	12%	9%	21%	13%
6	25%	10%	18%	9%	7%	18%	12%
7	23%	9%	18%	9%	7%	18%	12%
<b>5</b>	<b>1.25</b>	<b>1.26</b>	<b>1.20</b>	<b>1.26</b>	<b>1.21</b>	<b>1.17</b>	<b>1.14</b>
<b>6</b>	<b>1.05</b>	<b>1.04</b>	<b>1.02</b>	<b>1.00</b>	<b>1.00</b>	<b>1.00</b>	<b>1.03</b>
<b>7</b>	<b>1.00</b>	<b>1.00</b>	<b>1.00</b>	<b>1.00</b>	<b>1.00</b>	<b>1.00</b>	<b>1.00</b>

Values were chosen for the  $C_m$ ,  $\lambda$ ,  $\beta$ ,  $\rho$ , in order to keep track of how the  $\psi$  values affect different methods, in the shaded part of the table, the values were divided by each other, to find the percentage of difference between each state. There is an increase in failure loads, when the fixation progresses from hinged state to fixed state.

## V. Conclusion

It was concluded that the frame element had better results than that of the layered shell element when compared to experimental works. In the parametric study, the shown results and graphs gives an overview of how various parameters control the slender columns behavior. Lastly, it was concluded that the Eurocode overestimated the capacity of the columns under the balance load, it assumes a constant curvature value under the balance load which is an incorrect assumption, the proposed method equation can be a suitable replacement, as it represents the correct column's behavior.

$$\phi = P/P_b * (\phi_b - \phi_f) + \phi_f \text{ in which } P \leq P_b$$

## References

- [1]. Committee, A. C. I. (2008). Building code requirements for structural concrete (ACI 318-08) and commentary.
- [2]. CSI, S. (2006). Ver. 10.07, integrated finite element analysis and design of structures basic analysis reference manual. Berkeley (CA, USA): Computers and Structures Inc.
- [3]. Embaby, A. (2014). Toward Rational Curvature of Reinforced Concrete Members. IABSE Symposium Report, 102(21), 1200–1207.
- [4]. Frost, P. (2011). Second order effects in RC columns: comparative analysis of design approaches. Masters thesis. Faculty of Engineering and Architecture Department of . . . .
- [5]. Institution, B. S. (2004). Eurocode 2: Design of concrete structures: Part 1-1: General rules and rules for buildings. British Standards Institution.
- [6]. Jenkins, Ryan W, & Frosch, J. R. (2015). Improved procedures for the design of slender structural concrete columns. Ph. D. thesis. Purdue University, USA.
- [7]. Jenkins, Ryan William. (2011). Analytical investigation of the stiffness of non-sway eccentrically loaded slender reinforced concrete columns. Purdue University.
- [8]. Rodrigues, E. A., Manzoli, O. L., Bitencourt Jr, L. A. G., dos Prazeres, P. G. C., & Bittencourt, T. N. (2015). Failure behavior modeling of slender reinforced concrete columns subjected to eccentric load. Latin American Journal of Solids and Structures, 12(3), 520–541.
- [9]. Silva, P. F., Sangtarashha, A., & Burgueño, R. (2012). P-Delta effects in limit state design of slender RC bridge columns. 15th WCEE World Conference on Earthquake Engineering, Lisbon, Portugal.
- [10]. Tikka, T. K. (2001). Examination of second-order effects in structural concrete columns and braced frames.
- [11]. Tikka, T. K., & Mirza, S. A. (2014). Effective length of reinforced concrete columns in braced frames. International Journal of Concrete Structures and Materials, 8(2), 99–116.
- [12]. Wytroval, T., & Tuchscherer, R. G. (2013). Design of Slender Concrete Columns. STRUCTURE Magazine, 10–13.
- [13]. Bidoli, A. (2017). Second Order Effects in Concrete Structures.
- [14]. Embaby, A. (2018). Estimated Secondary Moments for Isolated Slender Reinforced Concrete Columns. Egypt.
- [15]. M.A. Farouk. (2017). Order Analysis in Braced Slender Columns, Part I: Approximate Equation for Computing the Additional Moments of Slender Columns.
- [16]. Hoyer, T. G., & Hansen, L. Z. (2002). Stability of Concrete Columns.

Ramez Raafat Sadek, et al. "Investigation of the Capacity of Braced Slender Reinforced Concrete Columns." *IOSR Journal of Mechanical and Civil Engineering (IOSR-JMCE)*, 17(2), 2020, pp. 44-57.